Topological properties of microwave magnetoelectric fields

M. Berezin, E. O. Kamenetskii, and R. Shavit

Microwave Magnetic Laboratory, Department of Electrical and Computer Engineering,
Ben Gurion University of the Negev,
Beer Sheva, Israel

Collective excitations of electron spins in a ferromagnetic sample dominated by the magnetic dipole-dipole interaction strongly influence the field structure of microwave radiation. A small quasi-two-dimensional ferrite disk with magnetic-dipolar-mode (MDM) oscillation spectra can behave as a source of specific fields in vacuum, termed magnetoelectric (ME) fields. A coupling between the time-varying electric and magnetic fields in the ME-field structures is different from such a coupling in regular electromagnetic fields. The ME fields are characterized by strong energy confinement at a subwavelength region of microwave radiation, topologically distinctive power-flow vortices, and helicity parameters [E. O. Kamenetskii, R. Joffe, and R. Shavit, Phys. Rev. E **87**, 023201 (2013)]. We study topological properties of microwave ME fields by loading a MDM ferrite particle with different dielectric samples. We establish a close connection between the permittivity parameters of dielectric environment and the topology of ME fields. We show that the topology of ME fields is strongly correlated with the Fano-resonance spectra observed at terminals of a microwave structure. We reveal specific thresholds in the Fano-resonance spectra appearing at certain permittivity parameters of dielectric samples. We show that ME fields originated from MDM ferrite disks can be distinguished by topological portraits of the helicity parameters and can have a torsion degree of freedom. Importantly, the ME-field phenomena can be viewed as implementations of space-time coordinate transformations on waves.

PACS number(s): 41.20.Jb, 42.25.Fx, 76.50.+g

I. INTRODUCTION

Interaction of electromagnetic radiation with topological singularities can result in strong transformation of the field structures. In this paper we report on the fundamentals of subwavelength confinement and symmetry breakings of microwave radiation via magnetic oscillations in small ferrite samples. Ferrite samples with linear dimensions smaller than the dephasing length of magnetic dipole-dipole interactions, but much larger than the exchange-interaction scales, are mesoscopic samples. In such samples one can observe collective excitations—the magnetic-dipolar-mode (MDM) [or magnetostatic (MS)] oscillations [1–4]. Recently, it was shown that MDM oscillations in a quasi-two-dimensional (quasi-2D) ferrite disk can conserve energy and angular momentum [5–8]. Because of these properties, MDMs are strongly coupled to microwave fields and enable us to confine microwave radiation energy in subwavelength scales. In a vacuum subwavelength region abutting a MDM ferrite disk one can observe the quantized-state power-flow vortices [9,10]. In such a region, a coupling between the time-varying electric and magnetic fields is different from such a coupling in regular electromagnetic (EM) fields. These specific fields, originated from MDM oscillations, we term magnetoelectric (ME) fields [11]. The ME-field solutions give evidence for spontaneous symmetry breakings at the resonant states of MDM oscillations. Because of rotations of localized field configurations in a fixed observer inertial frame, the linking between the EM and ME fields cause violation of the Lorentz symmetry of space-time. In such a sense, ME fields can be considered as Lorentz-violating extension of the Maxwell equations [12,13].

To characterize the ME-field singularities, the helicity parameter was introduced. A time average helicity parameter

for the near fields of a ferrite disk with MDM oscillations is defined as [11,14,15]

$$F = \frac{1}{16\pi} \text{Im}\{\vec{E} \cdot (\vec{\nabla} \times \vec{E})^*\}. \tag{1}$$

One can also introduce a normalized helicity parameter, which shows a time-averaged space angle between rotating vectors $\vec{E}$ and $\vec{\nabla} \times \vec{E}$:

$$\cos\alpha = \frac{\text{Im}\{\vec{E} \cdot (\vec{\nabla} \times \vec{E})^*\}}{|\vec{E}||\nabla \times \vec{E}|}. \tag{2}$$

In the regions where this parameter is not equal to zero, a space angle between the vectors $\vec{E}$ and $\vec{\nabla} \times \vec{E}$ is not equal to 90°. This breaks the field structure of Maxwell electrodynamics.

Topological structure of ME fields results in specific interactions of such fields with external EM fields. With the helicity properties of the fields, observed in a vacuum or isotropic-dielectric region abutting a quasi-2D ferrite disk with the MDM oscillations, one becomes faced with fundamental aspects akin to the problems of axion electrodynamics. Maxwell's equations are invariant when the electric and magnetic fields mix via rotation by an arbitrary angle ξ. For a real angle ξ, such a duality symmetry leaves invariant quadratic forms for the fields. This symmetry can be extended to Maxwell's equations in the presence of sources, provided that additional magnetic charges and currents are introduced [16]. MDM ferrite disks appear as pseudo-scalar particles [8,11]. The helicity density, defined by Eq. (1) or Eq. (2), transforms as a pseudo-scalar under space reflection P and it is odd under time reversal T. Whenever a pseudo-scalar axionlike field ϑ is introduced in the theory, the dual symmetry is spontaneously and explicitly broken. An axion-electrodynamics term, added to the ordinary

Maxwell Lagrangian [17],

$$\mathcal{L}_\vartheta = \kappa \vartheta \vec{E} \cdot \vec{B}, \tag{3}$$

where κ is a coupling constant, results in modified electrodynamics equations with the electric charge and current densities replaced by [17,18]

$$\rho^{(e)} \to \rho^{(e)} + \kappa \vec{\nabla} \vartheta \cdot \vec{B}, \tag{4}$$

$$\vec{j}^{(e)} \to \vec{j}^{(e)} - \kappa \left(\frac{\partial \vartheta}{\partial t} \vec{B} + \vec{\nabla} \vartheta \times \vec{E} \right). \tag{5}$$

Integrating Eq. (3) over a closed space-time with periodic boundary conditions, we obtain the quantization

$$S_\vartheta = \int \mathcal{L}_\vartheta \, d^4 x = \vartheta n, \tag{6}$$

where n is an integer. It is evident that S_ϑ is a topological term. While S_ϑ generically breaks the parity and time-reversal symmetry, both symmetries are intact at $\vartheta = 0$ and $\vartheta = \pi$. The field ϑ itself is gauge dependent.

Long radiative lifetimes of MDMs combine strong subwavelength confinement of electromagnetic energy with a narrow spectral linewidth. Due to these effects, MDMs may carry the signature of Fano resonances. An interest in observing and analyzing Fano profiles is driven by their high sensitivity to the details of the near-field scattering process. The Fano-interference effects in microwave scattering by a MDM ferrite particle were shown in Refs [15,19–21]. It is very important to note that the observed multiresonance spectrum of MDM oscillations has an evident analogy with the Fano-interference spectra in semiconductor quantum dots [22]. The MDM Fano resonances exhibit very strong sensitivity to changes of the local environment and so could be very informative in study of properties of ME fields. As the local environment with varying parameters, different dielectric samples abutting a ferrite disk can be used. In the previous studies, it was shown that there exists strong interaction of MDM oscillations with dielectric samples. It was found that due to such dielectric loadings we have widening of the MDM spectrum and shift the spectrum to lower frequencies. In the former case, the effect is due to specific electric fluxes, which are created by topological-phase magnetic currents on a lateral surface of a ferrite disk [7,8,11,19]. In the latter case, the effect is due to reduction of the Larmor frequency of a ferrite structure [11,15]. It was also shown that inside a dielectric loading, the helicity properties of the fields, originating from a MDM ferrite disk, are in strong dependence of permittivity of a dielectric material [11,15].

In the present work we study topological properties of microwave ME fields based on analyses of interaction of a MDM ferrite particle with dielectric environment. For this purpose we load a MDM ferrite particle by dielectric samples having the same geometry but different permittivity parameters. Because of strong coupling between the EM and ME fields in dielectrics, we are able to establish a close connection between the permittivity parameters of dielectric samples and topology of ME fields. We show that a character of

the local matter-field interaction is strongly correlated with the far-field responses observed in the Fano-resonance spectrum. We reveal that for an entire spectrum, the shape of Fano resonances is different for MDMs having different azimuth numbers. We observe strong overlapping of Fano resonances. Merging of two resonances results in the appearance of so-called "Fano quadrupoles" [23–25]. The physics of interaction of a MDM ferrite particle with the environmental microwave radiation and matter become clearer when one analyzes the helicity properties of the ME fields. We show that for different permittivities of dielectric loadings, ME fields originated from MDM ferrite disks can be distinguished by topological portraits of the helicity parameters. Also we show that ME fields can be characterized by helical topological loops and can have a torsion degree of freedom. In Refs. [7,8,11], we theoretically predicted that because of the double-helix resonances of MDM oscillations in a ferrite disk, the near fields of a particle can have such topology. In the present paper we numerically reveal these topological characteristics of the fields.

The paper is organized as follows. In Sec. II we give a brief theoretical insight into the origin of MDM oscillations and their interaction with dielectric samples. In Sec. III we present the results of our studies. We show the effects of Fano-resonance transformations at variation of permittivity parameters of dielectric environment and analyze topological properties of ME fields based on portraits of the helicity parameters and structures of the electric and magnetic fields. We show that for ME fields the torsion degree of freedom can exist. Section IV is devoted to discussions of the observed nontrivial topological properties of microwave ME fields. The main aspect of these discussions concerns the issue that helicity of the ME field is correlated with the space-time curvature. Section V summarizes our results.

II. THEORETICAL INSIGHT INTO ORIGIN OF MDM OSCILLATIONS AND THEIR INTERACTION WITH DIELECTRIC ENVIRONMENT

Studies of the spectrum transformations and field structures in dielectric samples loading a ferrite disk allow revealing topological properties of microwave ME fields originated from MDM oscillations. This is a basic idea, used in the present paper. From a general consideration it is known, however, that magnetization dynamics in homogeneous magnetic materials with structural symmetry cannot influence the dynamics of electric polarization [1]. Therefore, a brief theoretical insight into the origin of MDM oscillations and their nontrivial interaction with dielectric samples is necessary.

For a spectral analysis of MDM oscillations in ferrite structures, so-called magnetostatic description is used. Physical justification of this description is based on the fact that in a small sample of a medium with strong temporal dispersion of the magnetic susceptibility, variation of electric energy is negligibly small and so the electric displacement current is negligibly small as well. In an analysis of such structures we should use three differential equations instead of the four-Maxwell-equation analysis of electromagnetic

fields [1–4,11]:

$$\nabla \cdot \vec{B} = 0, \tag{7}$$

$$\vec{\nabla} \times \vec{E} = -\frac{1}{c}\frac{\partial \vec{B}}{\partial t}, \tag{8}$$

$$\vec{\nabla} \times \vec{H} = 0. \tag{9}$$

Taking into account a constitutive relation

$$\vec{B} = \vec{H} + 4\pi\vec{m}, \tag{10}$$

where $\vec{m}$ is the magnetization, one obtains from Eq. (7):

$$\vec{\nabla} \cdot \vec{H} = -4\pi\vec{\nabla} \cdot \vec{m}. \tag{11}$$

This presumes an introduction of MS-potential wave functions $\psi(\vec{r},t)$ for description of a magnetic field:

$$\vec{H} = -\vec{\nabla}\psi. \tag{12}$$

The spectral problem is formulated for MS-potential wave functions $\psi(\vec{r},t)$, where a magnetization field is expressed as

$$\vec{m} = -\ddot{\chi} \cdot \vec{\nabla}\psi. \tag{13}$$

Here $\ddot{\chi}$ is the susceptibility tensor [1–4]. Formally, in a system of Eqs. (7)–(9), a potential magnetic field and a curl electric field should be considered as completely uncoupled fields. No sensitivity to dielectric properties of materials is presumed in this case. It turns out, however, that the magnetic and electric fields in Eqs. (7)–(9) can be united and also the sensitivity to dielectric properties of materials can take place. It was found that in a case of a quasi-2D ferrite disk, the spectral-problem solution for MDM oscillations shows the presence of the unified (electric and magnetic) field structure which is different from the Maxwell-electrodynamics unified-field structure. We term the fields originated from the MDM oscillations as magnetoelectric (ME) fields to distinguish them from regular electromagnetic (EM) fields [11]. It was also shown that MDM oscillations in a quasi-2D ferrite disk can be sensitive to dielectric loadings [15,19].

MDM oscillations in a quasi-2D ferrite disk are mesoscopically quantized states. Long-range dipole-dipole correlation in position of electron spins in a ferromagnetic sample can be treated in terms of collective excitations of the system as a whole. If the sample is sufficiently small so that the dephasing length L_{ph} of the magnetic dipole-dipole interaction exceeds the sample size, this interaction is nonlocal on the scale of L_{ph}. This is a feature of mesoscopic ferrite samples, i.e., samples with linear dimensions smaller than L_{ph} but still much larger than the exchange-interaction scales. In a case of a quasi-2D ferrite disk, the quantized forms of these collective matter oscillations—magnetostatic magnons—were found to be quasiparticles with both wavelike and particlelike behavior, as expected for quantum excitations. The magnon motion in this system is quantized in the direction perpendicular to the plane of a ferrite disk. The MDM oscillations in a quasi-2D ferrite disk, analyzed as spectral solutions for the MS-potential wave function $\psi(\vec{r},t)$, have evident quantumlike attributes [5–8,11]. Analytically, there are two spectral models for the MDM oscillations in a ferrite disk. These models are

based on the so-called G- and L-mode spectral solutions. For G modes one has the Hermitian Hamiltonian for MS-potential wave functions $\psi(\vec{r},t)$. These modes are related to the discrete energy states of MDMs. In a case of the L modes, there is a complex Hamiltonian for MS-potential wave functions $\psi(\vec{r},t)$. For eigenfunctions associated with such a complex Hamiltonian, we have a nonzero Berry potential (meaning the presence of geometric phases). The main difference between the G- and L-mode solutions becomes evident when one considers the boundary conditions on a lateral surface of a ferrite disk. In solving the energy-eigenstate spectral problem for the G-mode states, the boundary conditions on a lateral surface of a ferrite disk are expressed as

$$\mu\left(\frac{\partial\tilde{\eta}}{\partial r}\right)_{r=\Re^-} - \left(\frac{\partial\tilde{\eta}}{\partial r}\right)_{r=\Re^+} = 0, \tag{14}$$

where $\tilde{\eta}$ is the G-mode MS-potential membrane wave function and $\Re$ is a radius of a ferrite disk. This boundary condition, however, manifests itself in contradictions with the electromagnetic boundary condition for a radial component of magnetic flux density $\vec{B}$ on a lateral surface of a ferrite-disk resonator. Such a boundary condition, used in solving the resonant spectral problem for the L-mode states, is written as

$$\mu(H_r)_{r=\Re^-} - (H_r)_{r=\Re^+} = -i\mu_a(H_\theta)_{r=\Re}, \tag{15}$$

where $(H_r)_{r=\Re^-}$ and $(H_r)_{r=\Re^+}$ are radial components of a magnetic field on a border circle, and $(H_\theta)_{r=\Re}$ is an azimuth magnetic field on a border circle. In the magnetostatic description, this equation appears as

$$\mu\left(\frac{\partial\tilde{\varphi}}{\partial r}\right)_{r=\Re^-} - \left(\frac{\partial\tilde{\varphi}}{\partial r}\right)_{r=\Re^+} = -\mu_a\nu(\tilde{\varphi})_{r=\Re^-}, \tag{16}$$

where $\tilde{\varphi}$ is the L-mode MS-potential membrane wave function, ν is an azimuth wave number, and μ_a is an off-diagonal component of the permeability tensor. The spectral-problem solutions based on Eq. (14) are single-valued-function solutions. At the same time, the spectral-problem solutions based on Eq. (16) are double-valued-function solutions. Because of the dependence of the right-hand side of Eq. (16) on a sign of the azimuth wave number, the two (clockwise and counterclockwise) types of resonant solutions may exist, in general, at a given direction of a bias magnetic field. As an example for the main MDM, in Fig. 1 we show the counterclockwise rotation of the MS-potential membrane wave function $\tilde{\varphi}$ inside a ferrite disk.

On a lateral border of a ferrite disk, the correspondence between a double-valued membrane wave function $\tilde{\varphi}$ and a single-valued function $\tilde{\eta}$ is expressed as $(\tilde{\varphi}_\pm)_{r=\Re^-} = \delta_\pm(\tilde{\eta})_{r=\Re^-}$, where $\delta_\pm \equiv f_\pm e^{-iq_\pm\theta}$ is a double-valued edge wave function on contour $\mathcal{L} = 2\pi\Re$ [7,8,11]. The azimuth number $q_\pm$ is equal to $\pm\frac{1}{2}l$, where l is an odd quantity ($l = 1, 3, 5, \dots$). For amplitudes we have $f_+ = -f_-$ and $|f_\pm| = 1$. Function $\delta_\pm$ changes its sign when θ is rotated by 2π so that $e^{-iq_\pm 2\pi} = -1$. As a result, one has the energy-eigenstate spectrum of MS-mode oscillations with topological phases accumulated by the edge wave function δ. On a lateral surface of a quasi-2D ferrite disk, one can distinguish two different functions $\delta_\pm$. A line integral around a singular contour $\mathcal{L}$, $\frac{1}{\Re}\oint_\mathcal{L}(i\frac{\partial\delta_\pm}{\partial\theta})(\delta_\pm)^*d\mathcal{L} = \int_0^{2\pi}[(i\frac{\partial\delta_\pm}{\partial\theta})(\delta_\pm)^*]_{r=\Re}d\theta$, is an observable quantity. It follows from the fact that owing to such a quantity one can restore
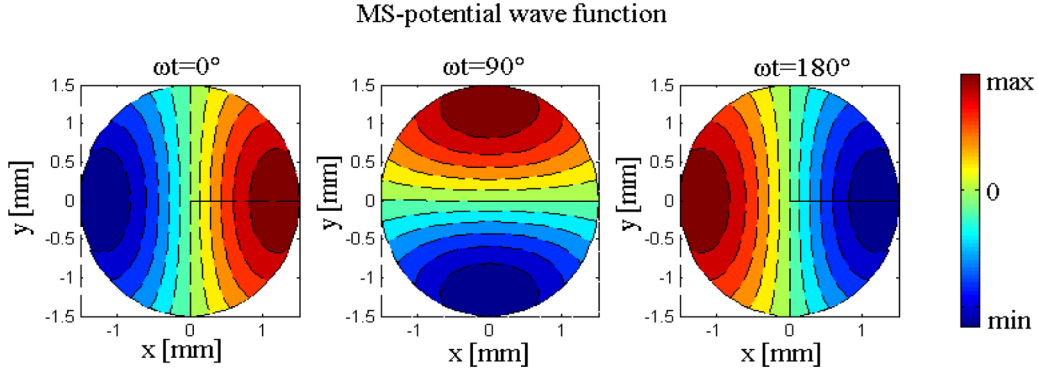
FIG. 1. (Color online) Rotating MS-potential membrane functions $\tilde{\varphi}$ inside a ferrite disk (arbitrary units).

single-valuedness (and, therefore, Hermicity) of the G-mode spectral problem. Because of a geometrical-phase factor on a lateral boundary of a ferrite disk, G modes are characterized by a pseudo-electric field (the gauge field) [7,8,11]. We denote this pseudo-electric field by the letter $\vec{\epsilon}$. The geometrical-phase factor in the G-mode solution is not single valued under continuation around a contour $\mathcal{L}$ and can be correlated with a certain vector potential $\vec{\Lambda}_{\epsilon}^{(m)}$ [7,8,11]:

$$i\Re \int_0^{2\pi} [(\vec{\nabla}_\theta \delta_\pm)(\delta_\pm)^*]_{r=\Re} d\theta \equiv K \oint_{\mathcal{L}} (\vec{\Lambda}_{\epsilon}^{(m)})_\pm \cdot d\vec{\mathcal{L}}$$
$$= 2\pi q_\pm, \qquad (17)$$

where $\vec{\nabla}_\theta \delta_\pm = \frac{1}{\Re} \frac{\partial \delta_\pm}{\partial \theta}|_{r=\Re} \vec{e}_\theta$ and $\vec{e}_\theta$ is a unit vector along an azimuth coordinate, and K is a normalization coefficient. In Eq. (17) we inserted a connection which is an analog of the Berry phase. In our case, the Berry's phase is generated from the broken dynamical symmetry. The confinement effect for magnetic-dipolar oscillations requires proper phase relation-ships to guarantee single-valuedness of the wave functions. To compensate for sign ambiguities and thus to make wave functions single valued we added a vector-potential-type term $\vec{\Lambda}_{\epsilon}^{(m)}$ (the Berry connection) to the MS-potential Hamiltonian. On a singular contour $\mathcal{L} = 2\pi\Re$, the vector potential $\vec{\Lambda}_{\epsilon}^{(m)}$ is related to double-valued functions. It can be observable

only via the circulation integral over contour $\mathcal{L}$, not pointwise. The field $\vec{\epsilon}$ is the Berry curvature. In contrast to the Berry connection $\vec{\Lambda}_{\epsilon}^{(m)}$, which is physical only after integrating around a closed path, the Berry curvature $\vec{\epsilon}$ is a gauge-invariant local manifestation of the geometric properties of the MS-potential wave functions. The corresponding flux of the gauge field $\vec{\epsilon}$ through a circle of radius $\Re$ is obtained as

$$K \int_S (\vec{\epsilon})_\pm \cdot d\vec{S} = K \oint_{\mathcal{L}} (\vec{\Lambda}_{\epsilon}^{(m)})_\pm \cdot d\vec{\mathcal{L}}$$
$$= K(\Xi^{(e)})_\pm = 2\pi q_\pm, \qquad (18)$$

where $(\Xi^{(e)})_\pm$ are quantized fluxes of pseudo-electric fields. There are the positive and negative eigenfluxes. These different-sign fluxes should be inequivalent to avoid the cancellation. It is evident that while integration of the Berry curvature over the regular-coordinate angle θ is quantized in units of 2π, integration over the spin-coordinate angle θ' ($\theta' = \frac{1}{2}\theta$) is quantized in units of π. The physical meaning of coefficient K in Eqs. (17), (18) concerns the property of a flux of a pseudo-electric field. It is related to the notion of a magnetic current used in the G-mode analysis. In Refs. [7,8], the coefficient K was conventionally taken as equal to unit. In
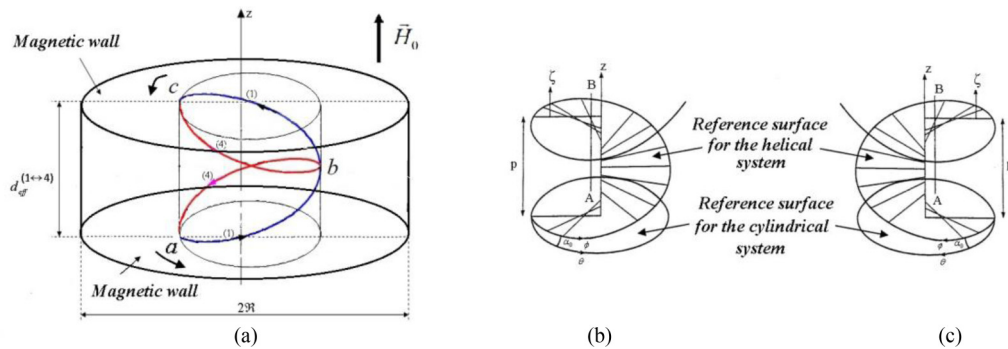

FIG. 2. (Color online) (a) Illustration of a double-helix resonance of MDM. The resonance appears when two magnetostatic helical modes [in particular, the modes (1) and (4) shown in the picture] create a closed loop. The dimension $d_{\text{eff}}^{(1\leftrightarrow4)}$ is equal to a pitch of helices. The azimuth phase over-running is characterized by the azimuth wave number $\nu = +1$. Arrows show directions of propagation for helical modes and a direction of rotation of a composition of helices. The helices are described based on the right-handed (b) and left-handed (c) Waldron's helical coordinate systems.
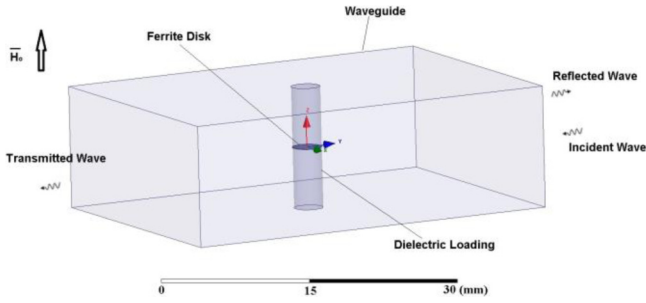
FIG. 3. (Color online) Rectangular waveguide with a MDM ferrite disk and loading dielectric cylinders.

FIG. 5. (Color online) Normalized reflection spectra without dielectric loading ($\varepsilon_r = 1$). Experimental results.

our recent study [11], we related quantity K to an elementary flux of the pseudo-electric field.

Due to the presence of quantized electric fluxes $\Xi^{(e)}$, we can observe multiresonance Fano-type spectrum of MDM oscillations. As we noted above, this spectrum strongly resembles the Fano-interference spectrum in semiconductor quantum dots [22]. While in Fano-resonance semiconductor quantum dots one has interference between the localized states and propagating electrons states via tunneling of discrete charges—electrons—into a dot, in a case of MDM ferrite disk this is because of quantized electric fluxes. Such quantized electric fluxes are well exhibited in an analysis of interaction of two coupled MDM ferrite disks [14,26]. In the Fano-resonance effects one has coupling between the quantized electric fluxes of a MDM ferrite disk and electric fields of EM waves propagating in a microwave structure.

The experimentally observed widening of the MDM spectrum at dielectric loading of a MDM disk is also due to the presence of quantized electric fluxes $\Xi^{(e)}$ [19]. At the same time, by virtue of such loading, one has low-frequency shifting of the MDM spectral peaks [11,15]. When an electrically polarized (due to the rf electric field of a microwave system) dielectric sample is placed above a ferrite disk, every separate dipole in this sample will precess around its own axis. Due to conservation of the total—spin plus orbital—angular momentum of varying magnetization at MDM resonances, one has induced mechanical torque acting on a dielectric body. The mechanical torque exerted on a given electric dipole is defined as a cross product of the MDM electric field and the electric moment of the dipole. In an entire macroscopic structure, complex evolution of magnetization moments (inside a ferrite disk)
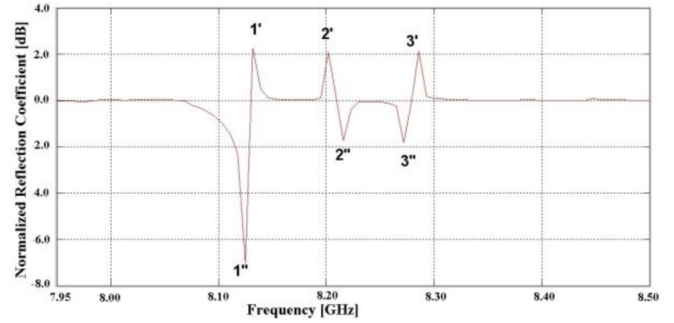
and electric dipole moments (inside a dielectric sample) should be at mechanical equilibrium. At MDM resonances, the torque exerting on the electric polarization in a dielectric should be equal to reaction torque exerting on the magnetization in a ferrite disk. Because of this reaction torque, the precessing magnetic moment density of the ferromagnet will be under additional mechanical rotation at a certain frequency Ω. For the magnetic moment density of the ferromagnet, $\vec{M}$, the motion equation [1–4] acquires the following form:

$$\frac{d\vec{M}}{dt} = -\gamma \vec{M} \times \left(\vec{H} - \frac{\Omega}{\gamma} \right), \qquad (19)$$

The frequency Ω is defined based on both spin and orbital momenta of the fields of MDM oscillations. One can see that at dielectric loadings, the magnetization motion in a ferrite disk is characterized by an effective magnetic field,

$$\vec{H}_{\text{eff}} = \vec{H} - \frac{\Omega}{\gamma}. \qquad (20)$$

Therefore, the Larmor frequency of a ferrite structure with a dielectric loading should be lower than such a frequency in an unloaded ferrite disk.

The L-mode analytical solutions, showing clockwise and counterclockwise rotations of MS-potential wave function, are obtained in a cylindrical coordinate system for a quasi-2D ferrite disk. From these solutions, one gets rotating electric and magnetic fields, power-flow vortices, and helicity parameters of MDMs [7,27,28]. Necessary justification of the L-mode spectrum is made from a general analysis of MS-potential wave functions $\psi(\vec{r},t)$ in a helical coordinate system [8].
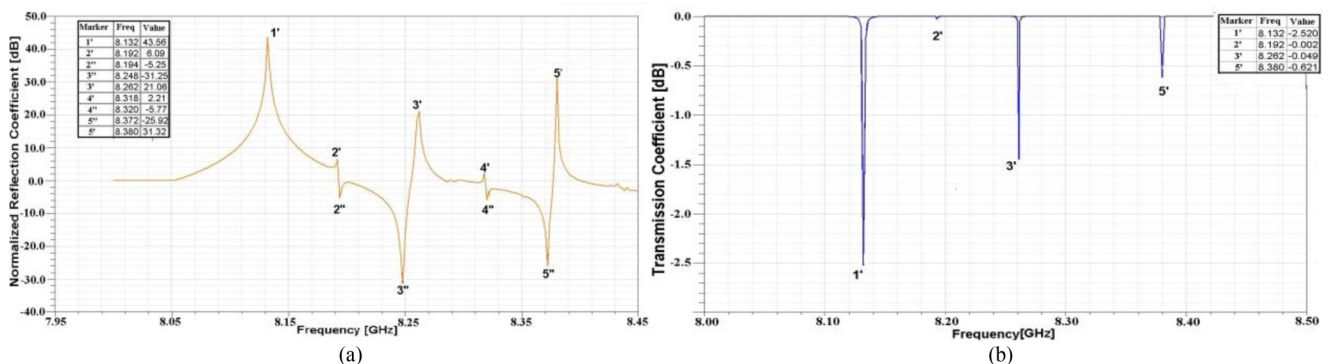

FIG. 4. (Color online) Normalized reflection and transmission spectra without dielectric loading ($\varepsilon_r = 1$). Numerical results.
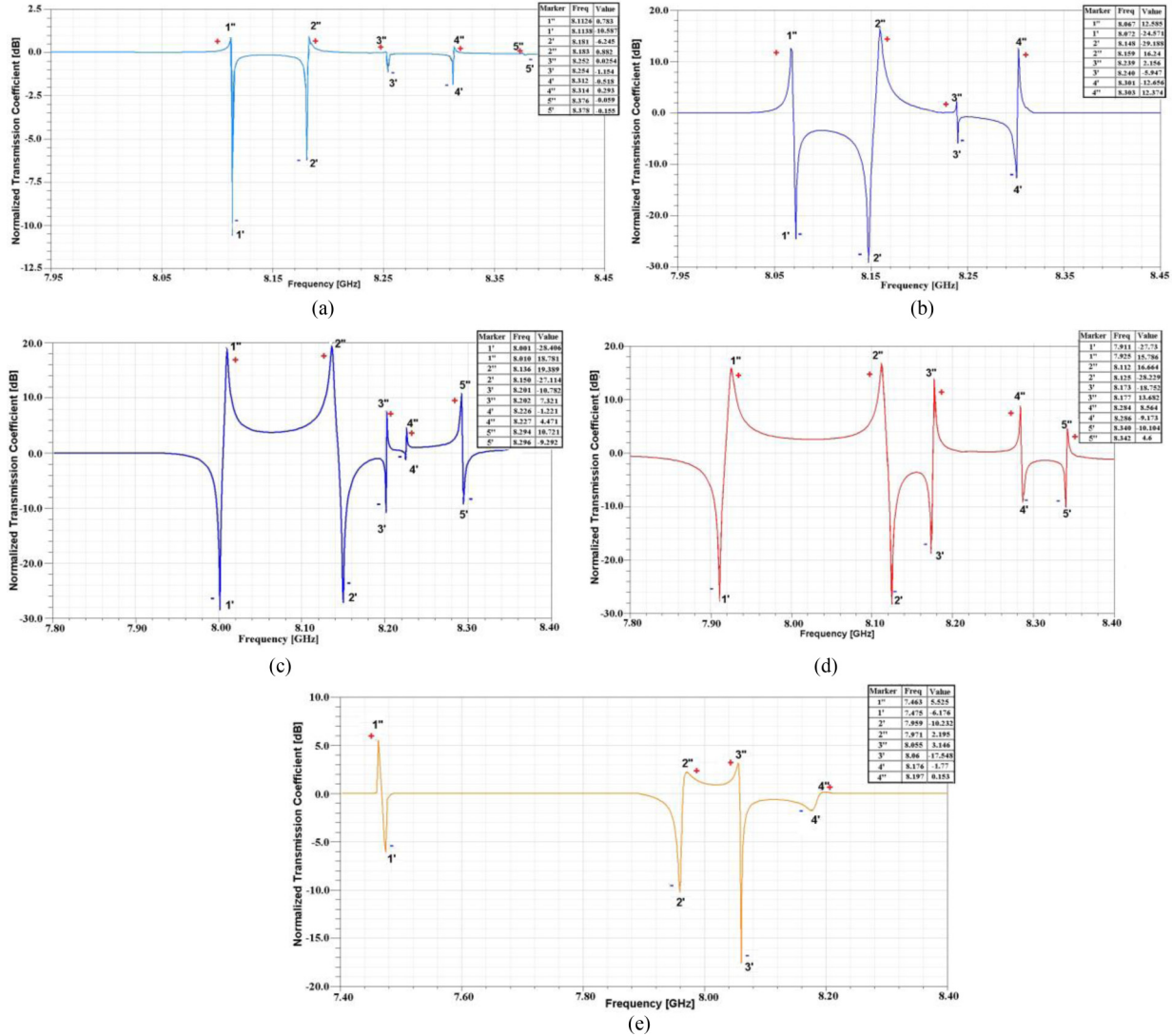
FIG. 6. (Color online) Numerically calculated normalized transmission spectra for different permittivity parameters of dielectric environment. (a) $\varepsilon_r = 10$; (b) $\varepsilon_r = 30$; (c) $\varepsilon_r = 50$; (d) $\varepsilon_r = 70$; (e) $\varepsilon_r = 100$.

This analysis shows that oscillations in a ferrite disk can be described by four helical modes. A pair of such interacting modes gives a double-helix resonance [8]. Figure 2 illustrates a double-helix resonance of MDMs which is described based on the right- and left-handed Waldron's helical coordinate systems [29]. This predetermines topological structures of ME fields: The magnetic and electric components of ME fields should have chiral properties. All the above properties of MDMs (rotating fields, power-flow vortices, and helicity parameters) are well modeled by numerical simulations when one considers the regions inside or near-field outside a quasi-2D ferrite disk [9–11,27,28]. There is difficulty, however, in showing numerically the helical-mode properties in regions far from a ferrite disk [10,14]. Thanks to use of dielectric samples abutting a ferrite disk, one has field localization in the regions far from a ferrite disk. In such a case, the helical-mode properties can be well shown numerically. For isotropic dielectric environment with sufficiently high permittivity, we observe double-helix resonances with chiral properties of the fields. This effect is shown in the results of the present studies.

III. RESULTS

A. MDM Fano resonances and helicity properties of ME fields

The structure of ME fields is strongly correlated with the Fano-resonance spectra observed at terminals of a microwave structure. Based on an analysis of transformations of the Fano-resonance spectra at variation of the permittivity parameters of dielectric samples, one can reveal topological characteristics of ME fields. In this section we show, both numerically and experimentally, such transformations of the Fano resonances. Our numerical studies are based on the HFSS electromagnetic simulation program (the software based on the finite-element method (FEM) produced by ANSYS Company). In a numerical analysis we use the yttrium iron garnet (YIG) disk of diameter of 3 mm. The disk thickness is 0.05 mm. The disk is normally magnetized by a bias magnetic field $H_0 = 4760$ Oe; the saturation magnetization of a ferrite is $4\pi M_s = 1880$ G. A ferrite disk is placed inside a TE_{10}-mode rectangular x-band waveguide symmetrically to its walls so that a disk axis is perpendicular to a wide wall

of a waveguide. The waveguide walls are made of a perfect electric conductor (PEC). For better understanding the field structures, in a numerical analysis we use a ferrite disk with a very small linewidth of $\Delta H = 0.1$ Oe. Two dielectric samples are cylinders of the same diameter as a ferrite disk—3 mm. The height of every cylinder corresponds to a distance from a disk surface to a waveguide wall and is about 6 mm. Figure 3 shows the structure under investigation. The microwave experiments are made with a ferrite disk having the same parameters, except for a parameter of magnetic losses. For a real disk we have a linewidth of $\Delta H = 0.8$ Oe. A thin dielectric substrate of a ferrite disk used in an experimental sample [the gadolinium gallium garnet (GGG) substrate with thickness of 0.5 mm] does not strongly influence the experimental results. In experiments we used dielectric cylinders of the same geometry made of microwave ceramics (TCI Ceramics Inc.): K-50 ($\varepsilon_r = 50$) and K-100 ($\varepsilon_r = 100$).

Figure 4 shows numerical results of the normalized reflection and transmission spectra for a ferrite without a dielectric loading ($\varepsilon_r = 1$). The normalization means that the spectra are represented with relation to the reflection (transmission) levels in a structure without a bias magnetic field. The designation of the resonance peaks is made in accordance with the mode classification used in Ref. [6]. From the digits n, one can know variations of MS-potential function in a ferrite disk with respect to azimuth and radial coordinates. Every odd digit corresponds to the modes with azimuth number 1. Every even digit corresponds to the modes with azimuth number 2. The number of radial variations can be found by the following scheme. For modes with $n = 1$ and $n = 2$, there is one radial variation (in accordance with Ref. [6], there are modes with $q = 1$). For modes with $n = 3$ and $n = 4$, one has two radial variations (in accordance with Ref. [6], there are modes with $q = 2$). For modes with $n = 5$ and $n = 6$, one has three radial variation (in accordance with Ref. [6], there are modes with $q = 3$), etc. So, the mode with $n = 1$ is the first radial and the first azimuthal mode, the mode with $n = 2$ is the first radial and the second azimuthal mode, the mode with $n = 3$ is the second radial and the first azimuthal mode, the mode with $n = 4$ is the second radial and the second azimuthal mode, etc. For a given number n, one prime means the reflection peak and double primes mean the transmission peak.

Without loading dielectrics ($\varepsilon_r = 1$), the transmission is strong and MDM resonances in a ferrite disk slightly interfere with microwave radiation passing through a waveguide. For this reason, one observes only the Lorentz-type resonances in the transmission spectrum. Contrarily, in the reflection response there is evidence for the Fano interference. The numerically obtained Fano resonances in the reflection spectrum are also well observed experimentally (see Fig. 5). It is worth noting here that while the first peak in the numerical reflection spectrum is a Lorentz-type resonance, such a peak in the experimental reflection spectrum is a Fano-type resonance. This difference in the peak forms is due to a specific excitation structure used in the experiment.

When dielectric samples load a ferrite disk, the reflection becomes strong and MDM resonances in a ferrite disk slightly interfere with backscattered microwave radiation. For this reason, the Fano-resonance effects are predominantly observed in the transmission spectra, but not in the reflection ones. In
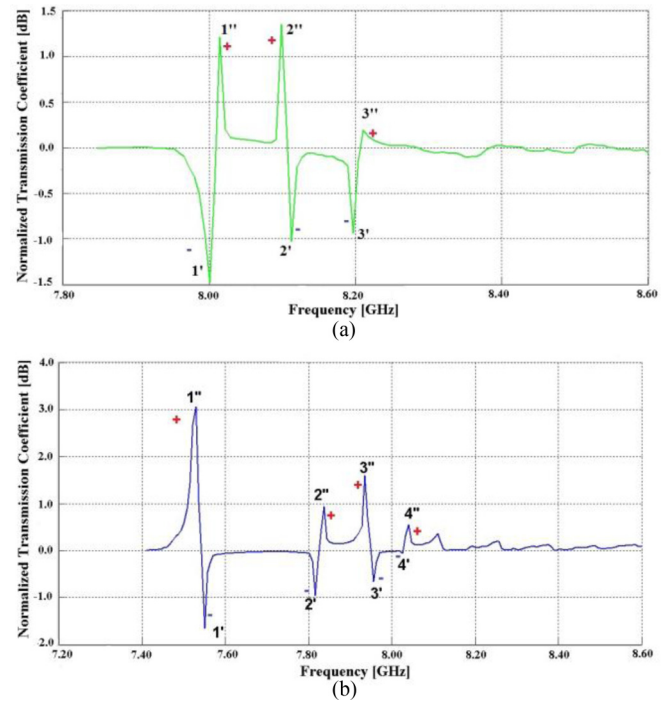

FIG. 7. (Color online) Normalized transmission spectra. Experimental results. (a) $\varepsilon_r = 50$; (b) $\varepsilon_r = 100$.

Fig. 6 we show the numerically calculated transmission spectra for different permittivity parameters of dielectric environment. Experimental results of the normalized transmission spectra for particular cases of dielectric samples with $\varepsilon_r = 50$ and $\varepsilon_r = 100$ are shown in Fig. 7. All these spectral pictures are in obvious correspondence with the above statement: With increase of permittivity of a dielectric loading, the distances between MDM spectral peaks increase as well. Also, one observes the low-frequency shifting of the MDM resonances. At the same time, very unusual effects of the Fano interference become evident. Evidently, for modes with different azimuth numbers (the modes designated, respectively, by odd and even digits n), the shape of Fano resonances is different. Since every peak of the Fano resonances in the transmission spectra has a positive and a negative pole with respect to a transmission
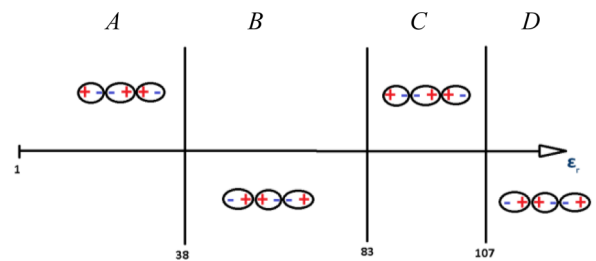

FIG. 8. (Color online) Fano dipoles for the first three resonances in the transmission spectra. The numbers show threshold quantities of the permittivity of dielectric samples. There are four regions of the permittivity parameters designated as A, B, C, and D. In every one of these regions, one has the same pictures of polarities of Fano dipoles.
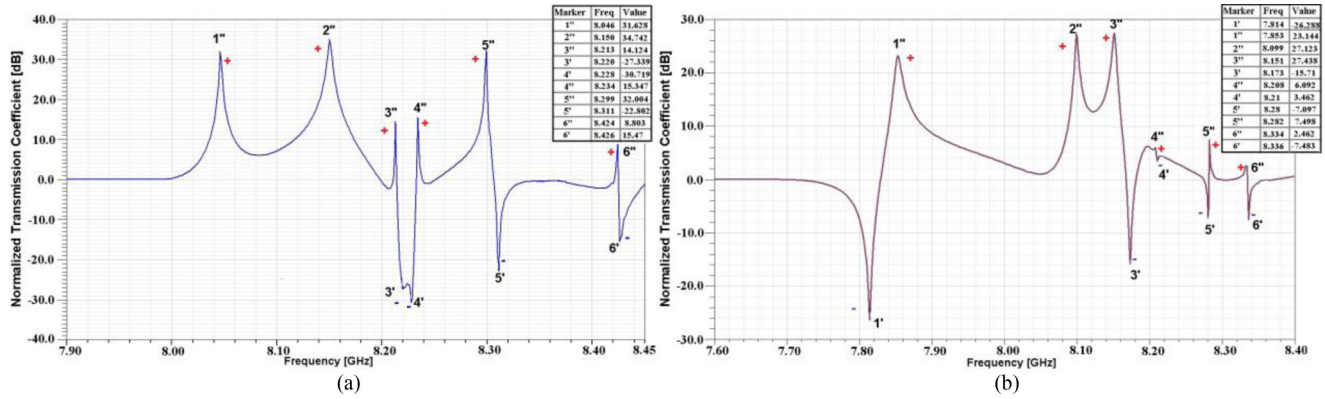
FIG. 9. (Color online) Lorentz-type resonances observed at thresholds of the permittivity parameters. (a) The threshold at $\varepsilon_r = 38$; (b) The threshold at $\varepsilon_r = 83$.

level in a structure without a bias magnetic field, we can say that for modes with different azimuth numbers there are opposite "polarities" of "Fano dipoles." At the same time, there are evident overlappings of Fano resonances. Merging of two resonances with opposite polarities results in the appearance of "Fano quadrupoles." These phenomena are similar to those observed in semiconductor quantum structures: When more than one resonant state is presented in a one-channel system, the resonance levels interact each other and result in the overlapping of resonances [23–25].

One of the most interesting effects of interaction of a MDM ferrite particle with dielectric environment is the presence of certain threshold quantities of the dielectric permittivity. At these thresholds, polarities of Fano dipoles alter and the shapes of Fano quadrupoles change. Figure 8 shows schematically orientations of Fano dipoles for the first three resonances in the transmission spectra with respect to the permittivity axis. The numbers are threshold permittivities of dielectrics. When crossing these thresholds, the polarity of Fano dipoles becomes opposite. As is shown in Fig. 8, for the transmission spectra there are four regions of the permittivity parameters designated as A, B, C, and D. Inside every one of these regions, one has the same pictures of polarities of Fano dipoles. The regions are separated by thresholds. The region A corresponds to dielectrics with $\varepsilon_r < 38$, the region B is bounded with $38 < \varepsilon_r < 83$, the region C is for $83 < \varepsilon_r < 107$, and the region D corresponds to dielectrics with $\varepsilon_r > 107$. In Fig. 9 one can see that exactly at the threshold permittivities the Lorentz-type resonances can appear.

Topology of the fields originated from a MDM particle—the ME fields—is well characterized by the helicity parameters described by Eq. (1) or (2). The helicity properties of the fields near a ferrite disk appear only at resonance frequencies of MDM oscillations. For different MDMs, one has different patterns of the helicity-parameter distributions. At nonresonant frequencies, the helicity parameter is zero [11,15]. Our preliminary study [11,15] showed that the helicity-parameter distributions can be very sensitive to the properties of dielectric environment. In the present paper we show that with transformation of an entire Fano-resonance spectrum via different dielectric loadings, one has strong variation of the helicity-parameter distributions. Moreover, the portraits of the

helicity-parameter distributions may give unique information on interaction of ME fields with dielectric matter. In Fig. 10, we show the normalized helicity parameters [calculated based on Eq. (2)] in correlation with the MDM spectra obtained at different dielectric loadings. The pictures are shown in the yz cross section of the structure (see Fig. 3). Analyzing these pictures one can come to an important conclusion. From Fig. 10, it appears that within every one of the regions of permittivity shown in Fig. 8, one has sufficiently similar portraits of the helicity parameters for MDM resonances designated by the same mode number n. For example, for MDMs with the same mode number n, there are very similar helicity portraits for $\varepsilon_r = 10$ and $\varepsilon_r = 30$ (in the permittivity region A), very similar portraits for $\varepsilon_r = 50$ and $\varepsilon_r = 70$ (in the permittivity region B), and very similar portraits for $\varepsilon_r = 100$ and $\varepsilon_r = 105$ (in the permittivity region C). Based on such a qualitative analysis we can conclude that for a given geometry of a dielectric sample, the threshold permittivity not only alters the pictures of polarities of Fano dipoles, but also changes the helicity portraits for selected resonances. The helicity portraits for the first and second Fano resonances, selected from Fig. 10, are shown in Fig. 11 at variation of the permittivity of the dielectric environment. As we can see, there is strong symmetry with respect to the disk axis for all the helicity portraits of the transmission peaks (peaks $1''$ and $2''$). At the same time, for the reflection peaks (peaks $1'$ and $2'$), the helicity portraits can be nonsymmetrical with respect to the disk axis. With variation of the permittivity of dielectric environment, one can observe nonsymmetry for the helicity factor or in vacuum regions outside dielectric cylinders, or inside dielectric cylinders. This effect shows us a "fine structure" of Fano resonances in microwave systems with embedded MDM ferrite disks. It is worth noting also that for peaks $2'$ and $2''$ we observe strong periodicity of the helicity parameters along an axis of a dielectric cylinder with high-quantity permittivities (for $\varepsilon_r = 100$ and $\varepsilon_r = 105$ in our studies). For large values of the permittivity, there is strong localization of EM energy inside a dielectric cylinder and at proper sizes of a dielectric sample we have standing EM waves along a cylinder axis. At the same time, the helicity property of ME fields is also essentially more exhibited in such dielectric loadings. As a result, we can observe a standing-wave behavior

of the ME and EM field interactions. A dielectric rod behaves as a torsion resonator with strong hybridization of the ME and EM states. The torsion degree of freedom for ME fields is well illustrated below by our numerical analysis. Figure 12 gives examples of distributions of the normalized helicity parameters on axis z (the cylinder axis) above and below the disk in vacuum and in a dielectric cylinder with $\varepsilon_r = 100$ for different MDM resonances. There is evident periodicity of the helicity parameter for the peak $2'$ at a dielectric load of $\varepsilon_r = 100$.

B. Torsion degree of freedom for ME fields

The properties of ME fields can be related to a so-called torsion degree of freedom—a subject of heightened interest in modern literature of the field structures. Torsion of space-time—coupling the time and the angular coordinates of the field—might be connected with the intrinsic angular momentum of matter. The torsion-structure fields can be created by ferromagnet structures with their intrinsic ordered spin motion. In the case of a ferromagnet, the spin motion
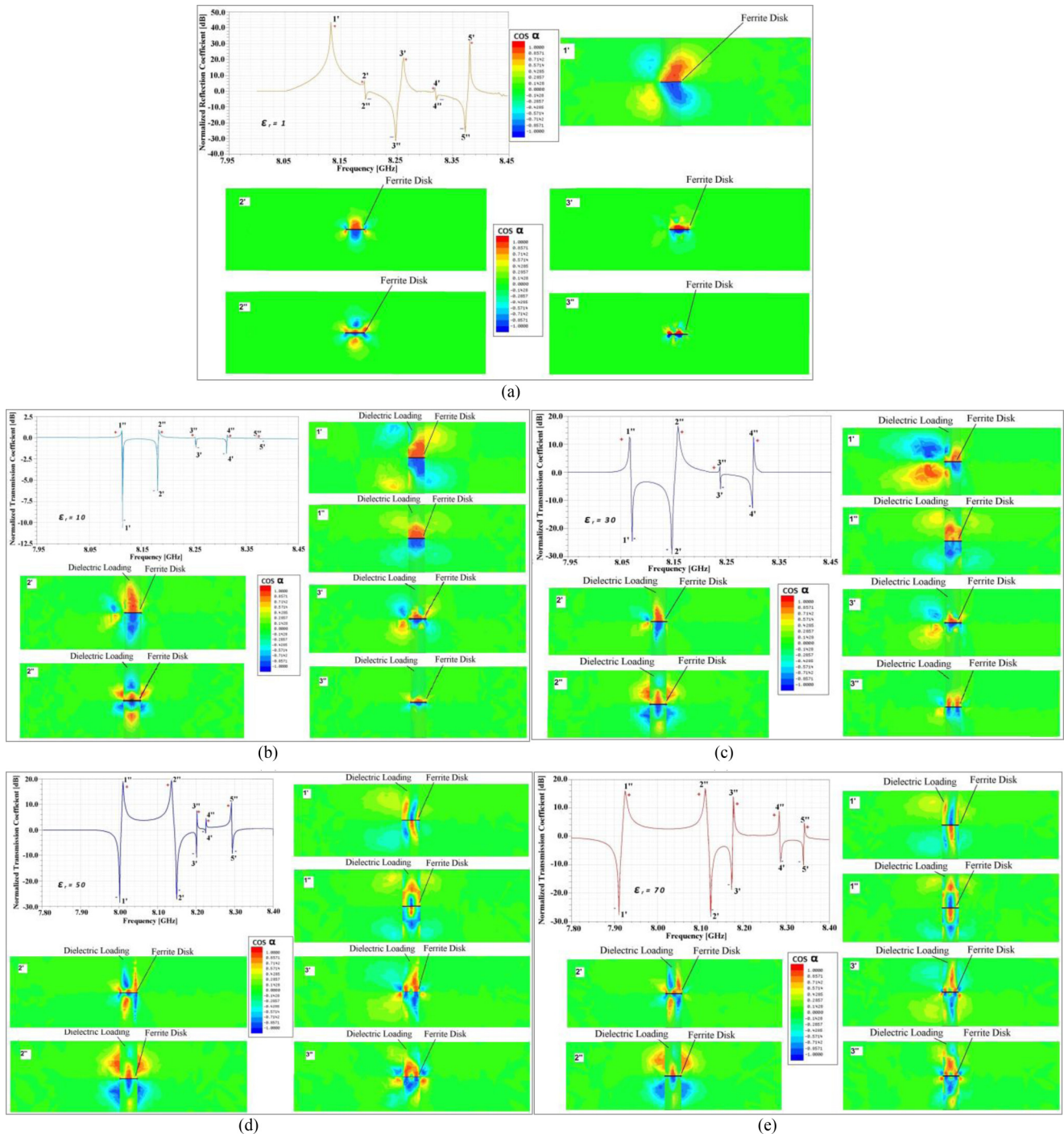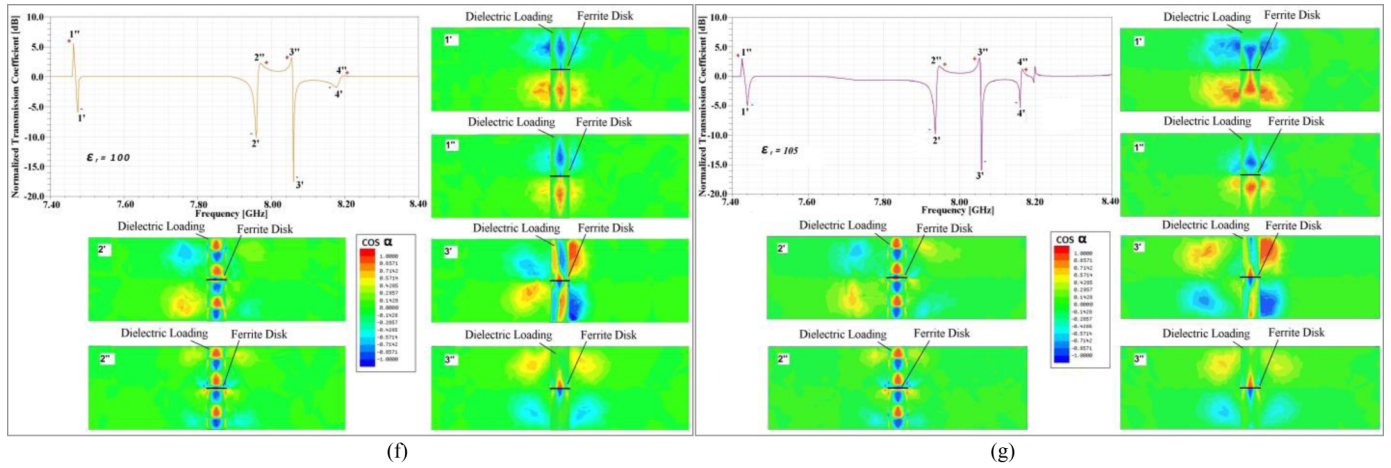

FIG. 10. (Color online) *(Continued.)*

FIG. 10. (Color online) The normalized helicity parameters represented in correlation with the MDM spectra obtained for different dielectric loadings. The pictures are shown in the yz cross section. (a) $\varepsilon_r = 1$; (b) $\varepsilon_r = 10$; (c) $\varepsilon_r = 30$; (d) $\varepsilon_r = 50$; (e) $\varepsilon_r = 70$; (f) $\varepsilon_r = 100$; (g) $\varepsilon_r = 105$.

originates from fermions ("spinor matter"). It is not possible to eliminate this motion through transition to a suitable rotating frame of reference. The spin angular momentum can be considered as the source of the fields which are inseparably coupled to the geometry of space-time [30–32]. However, the effects of torsion in a gravitational context are very negligible, experimentally [31,32]. At the same time, it is shown that condensed matter systems can provide useful laboratories for the study of torsion. Solid and liquid crystals with topological defects in the continuum limit can also be described by a manifold where the curvature and torsion fields are proportional to the topological charge densities of the defects [33,34]. In uniform plasmas one can observe a torsional Alfvén mode. There is a twisting of magnetic field lines forming a concentric flux shell [35]. One of important aspects of the torsion degree of freedom concerns a torsion
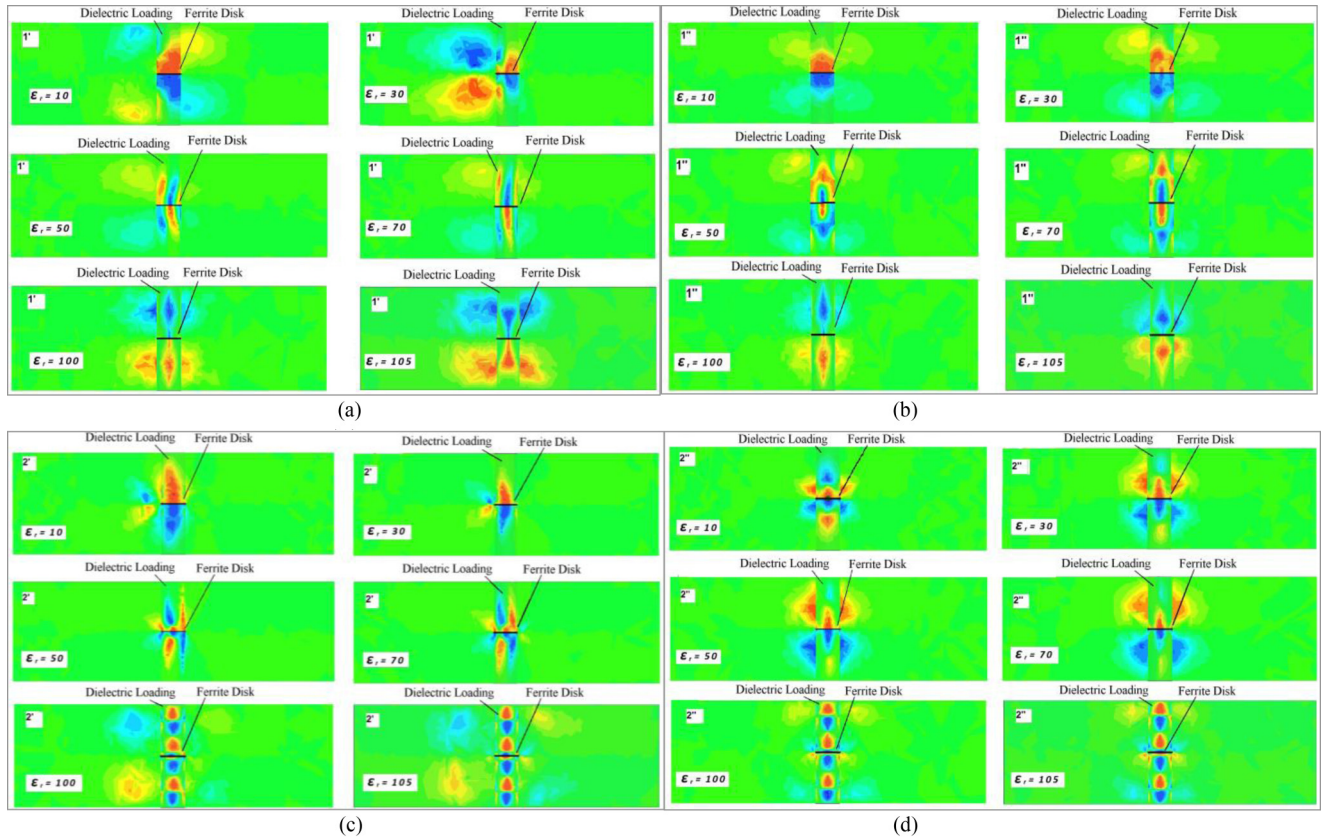

FIG. 11. (Color online) The helicity portraits for the first and second Fano resonances at variation of the permittivity of the dielectric environment. The pictures are shown in the yz cross section. (a) Reflection peak for the first Fano resonance (peaks $1'$); (b) transmission peak for the first Fano resonance (peak $1''$); (c) reflection peak for the second Fano resonance (peak $2'$); (d) transmission peak for the second Fano resonance (peak $2''$).
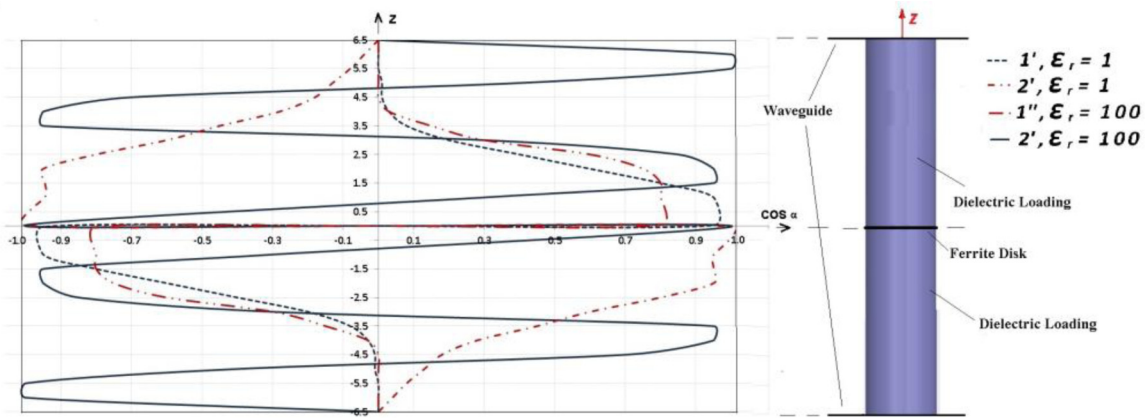
FIG. 12. (Color online) Distributions of the normalized helicity parameters on axis z (the cylinder axis) above and below a ferrite disk in vacuum and in a dielectric cylinder ($\varepsilon_r = 100$) for different MDM resonances.
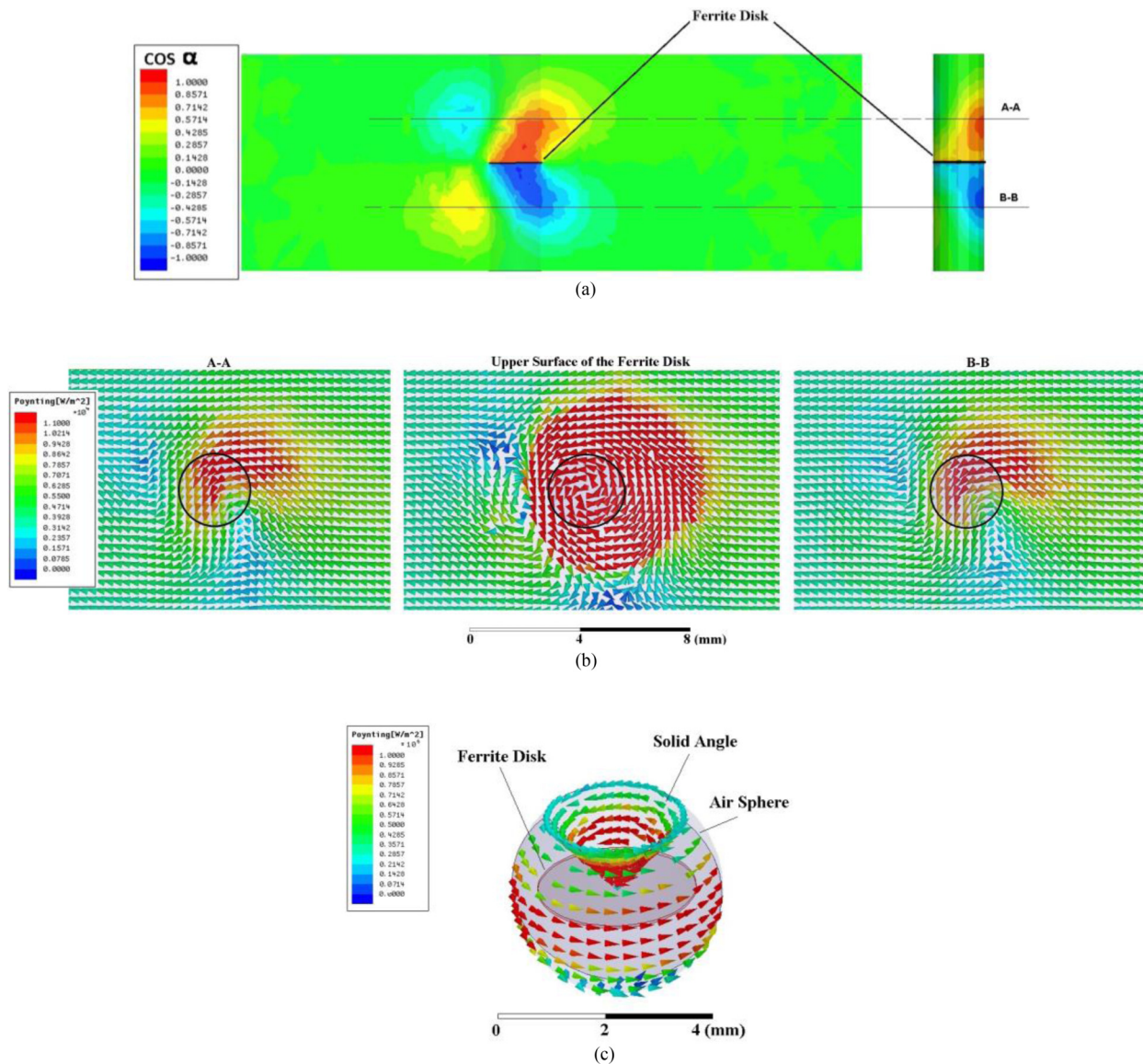

FIG. 13. (Color online) The field structure outside a ferrite disk for the first MDM resonance (resonance peak 1′) at vacuum environment ($\varepsilon_r = 1$). (a) Normalized helicity parameter shown on the yz cross-section plane and on a lateral surface of a vacuum cylinder ($\varepsilon_r = 1$) having the same geometry as loading dielectric cylinders. (b) Power-flow distributions on vacuum planes A-A, B-B, and immediately above a ferrite disk. (c) Circulation and divergence of the power flow shown on a surface of a vacuum sphere and on a surface of a solid angle.
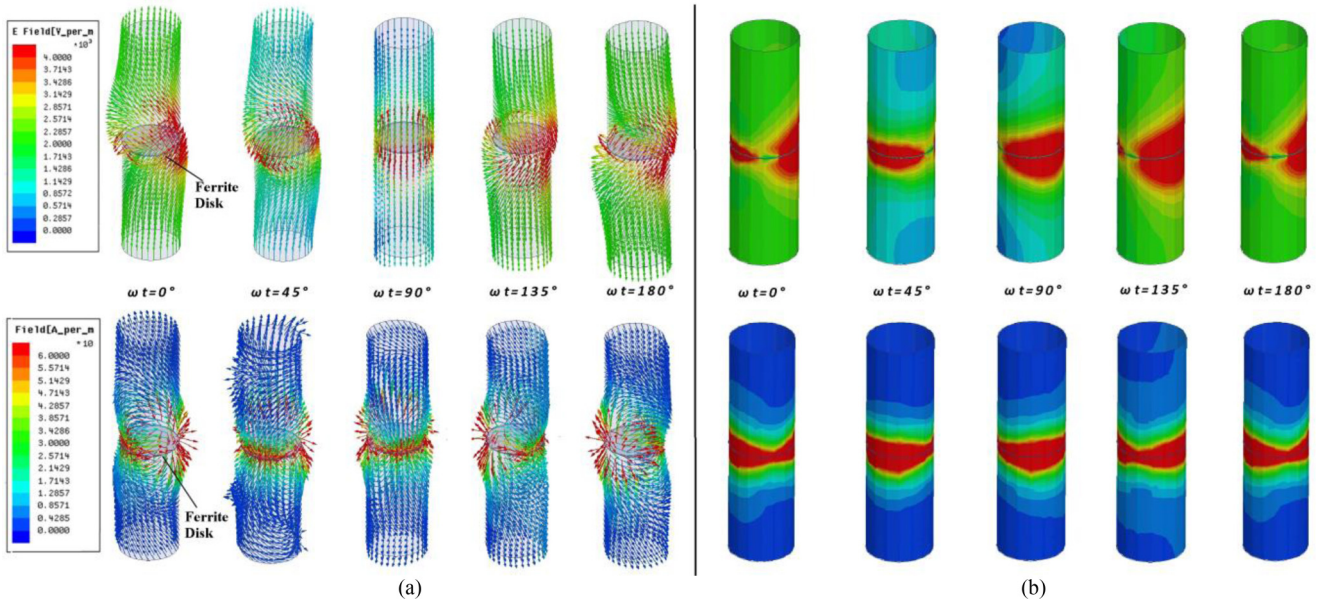
FIG. 14. (Color online) Structures of the electric and magnetic fields on a lateral surface of a vacuum cylinder ($\varepsilon_r = 1$) above and below a ferrite disk for the first reflection peak (peak 1′). (a) Field vectors; (b) field magnitudes.

contribution to helicity [36]. Due to the intrinsic angular momentum of spinor matter and long-range phase coherence in magnetic dipole-dipole interactions between a pair of spins, a quasy-2D ferrite disk with MDM oscillations can behave as a torsional defect for propagating-wave EM fields. Existence of a torsion degree of freedom can be considered as one of the most important distinctive features of the ME fields created by MDM particles. A question on a torsion degree of freedom of ME fields may arise from the double-helix resonances of MS-potential wave functions $\psi(\vec{r},t)$ [8]. Also the presence of spin and orbital angular momenta of the MDM fields (and so, the presence of power-flow vortices) inside a ferrite disk [27,28] makes evident the necessity for external varying fields of a microwave structure to behave with certain angular momenta and power-flow vortices. Otherwise, the system will be out of an equilibrium state. In a case of vacuum environment, these external-field angular momenta and power-flow vortices are distributed around the entire microwave system. However, for dielectric loads, the external-field angular momenta and

power-flow vortices can be mostly localized inside a dielectric. In this case, one can observe unique pictures of the fields with a torsion degree of freedom.

We start with an illustration of a structure of ME fields for vacuum environment. Then, we will show that with use of a dielectric loading cylinder, good verification of the double-helix-resonance behavior and the torsion degree of freedom of ME fields can be obtained. Figure 13 shows power flows of the ME fields on different surfaces in vacuum for the first reflection peak (peak 1′). These pictures are correlated with the helicity portraits, which are shown on the yz cross-section plane and on a lateral surface of a vacuum cylinder ($\varepsilon_r = 1$) having the same geometry as loading dielectric cylinders. There is a strong power-flow vortex on a vacuum plane immediately above a ferrite disk. Declination of the power flow from a regular power-flow way in a waveguide without a ferrite disk is in evident correlation with declinations in the helicity-parameter distribution. One observes circulation and divergence of the power flow far from a ferrite disk. A topological structure
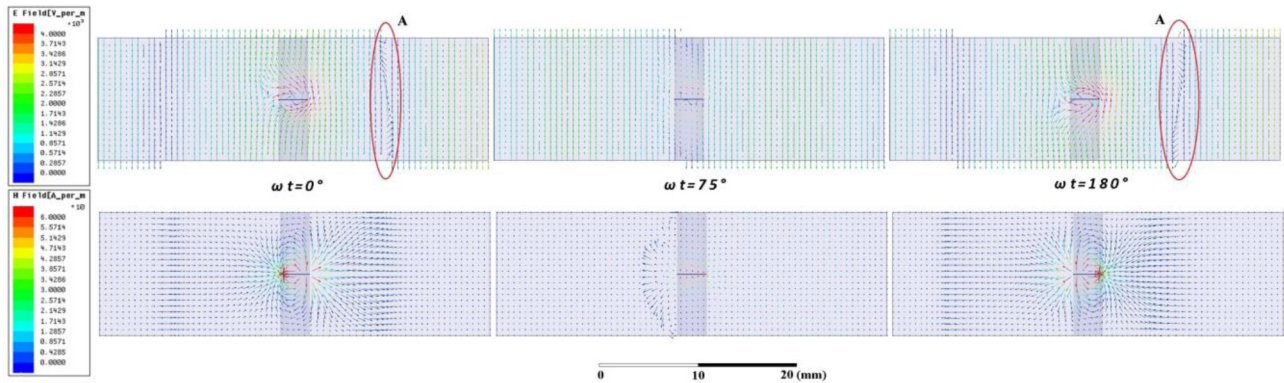

FIG. 15. (Color online) Structures of the electric and magnetic fields for the first reflection peak (peak 1′) on the yz cross-sectional plane. A vacuum cylinder ($\varepsilon_r = 1$) is shown as a highlighted area. A helical structure of a ME field is evident in regions A at phases when an electric field of incident microwave radiation is zero.
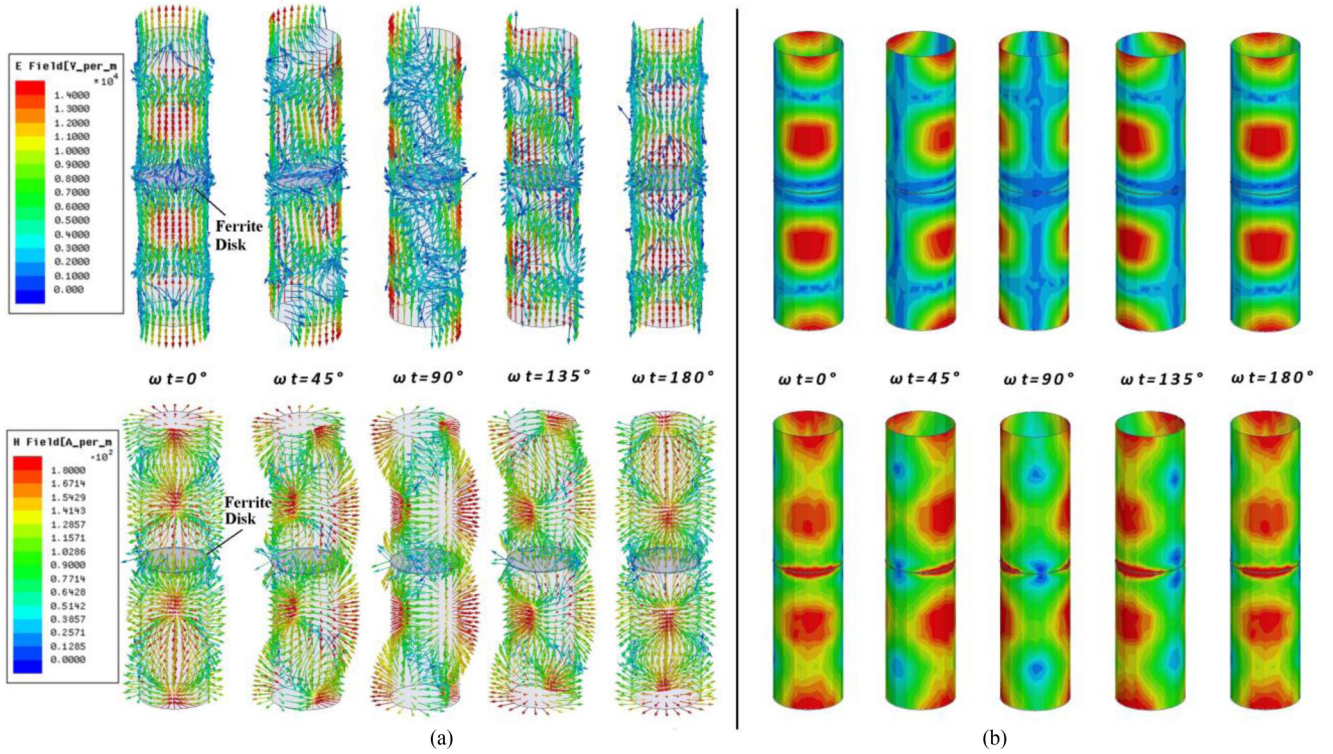
FIG. 16. (Color online) Structures of the electric and magnetic fields on a lateral surface of a dielectric cylinder ($\varepsilon_r = 100$) above and below a ferrite disk for the second transmission peak (peak $2''$). (a) Field vectors; (b) field magnitudes.

of the field in vacuum environment is also well illustrated by distribution of power flow on a surface of a vacuum sphere surrounding a ferrite disk and inside a solid angle in this sphere. In Fig. 14, we show structures of the electric and magnetic fields on a lateral surface of a vacuum cylinder ($\varepsilon_r = 1$) for different time phases. Both the electric and magnetic fields are strongly concentrated in the vicinity of a ferrite disk. The fields have the azimuth and axial phase variations. The fields rotate and the direction of rotation depends on the direction of a bias magnetic field. In the field-vector pictures one can see the rotating crests. Obviously, the fields have a helical structure. Moreover, there is evidence for double-helix resonances [8]. Figure 15 shows the electric and magnetic fields on the yz cross-sectional plane. A vacuum cylinder ($\varepsilon_r = 1$) is shown as a highlighted area. In regions where the phases of an electric field of incident microwave radiation is zero, one can clearly see helical structures of a ME field. In Fig. 15, these regions are denoted by a capital letter A.

Because of exponential decay of ME fields along the z axis, above and below a ferrite disk, the helical structures of the fields in vacuum are exhibited very slightly. This behavior becomes more evident when dielectric cylinders load a ferrite disk. Figure 16 shows structures of the electric and magnetic fields on a lateral surface of a dielectric cylinder ($\varepsilon_r = 100$) for the second transmission peak (peak $2''$). In double-helix resonances, there are interactions of two helical modes (one is a right-handed helix and the other is a left-handed helix) resulting in the appearance of rotating helical crests. These helical crests are clearly seen in Fig. 16(a). Figure 17 shows a distribution of the power-flow vortices along a dielectric cylinder. These distributions are correlated with the helicity

portraits, which are shown on the yz cross-section plane and on a lateral surface of the loading dielectric cylinder. In comparison with a picture of the power-flow distribution in vacuum environment (see Fig. 13), in the case of a dielectric load with a high value of permittivity, the power-flow vortices are strongly localized inside a dielectric cylinder. One can see that, for the second transmission peak (peak $2''$), all the vortices have the same direction of rotation along a cylinder axis. This situation can be different for another resonance. Figure 18 shows an axial distribution of the power flow on a lateral surface of a dielectric cylinder ($\varepsilon_r = 100$) for the first transmission peak (peak $1''$). In this case, the power-flow vortices have different directions of rotations along a cylinder axis. This is an additional evidence for a torsion degree of freedom of ME fields.

IV. DISCUSSION

In Maxwell electrodynamics, a spatial geometry is the Euclidian geometry. In Euclidean space the electric-field and magnetic-field energies are additive (and hence independent) quantities. We have the energy density for EM field: $w_{\mathrm{EM}} = \frac{1}{8\pi}(|\vec{E}|^2 + |\vec{H}|^2) = \mathrm{const}$ in any point in vacuum. In isotropic dielectric space, there is $w_{\mathrm{EM}} = \frac{1}{8\pi}(\varepsilon|\vec{E}|^2 + |\vec{H}|^2) = \mathrm{const}$.

Recent metamaterial implementations facilitate space-time transformations in the electromagnetic-field structure. A physical means to control electromagnetic waves by using artificial composites is based on the invariance of Maxwell's equations under a general coordinate transformation [37,38]. The ME field, studied in this paper, is correlated with the space-time curvature. Normalized helicity of a ME field is a time-averaged
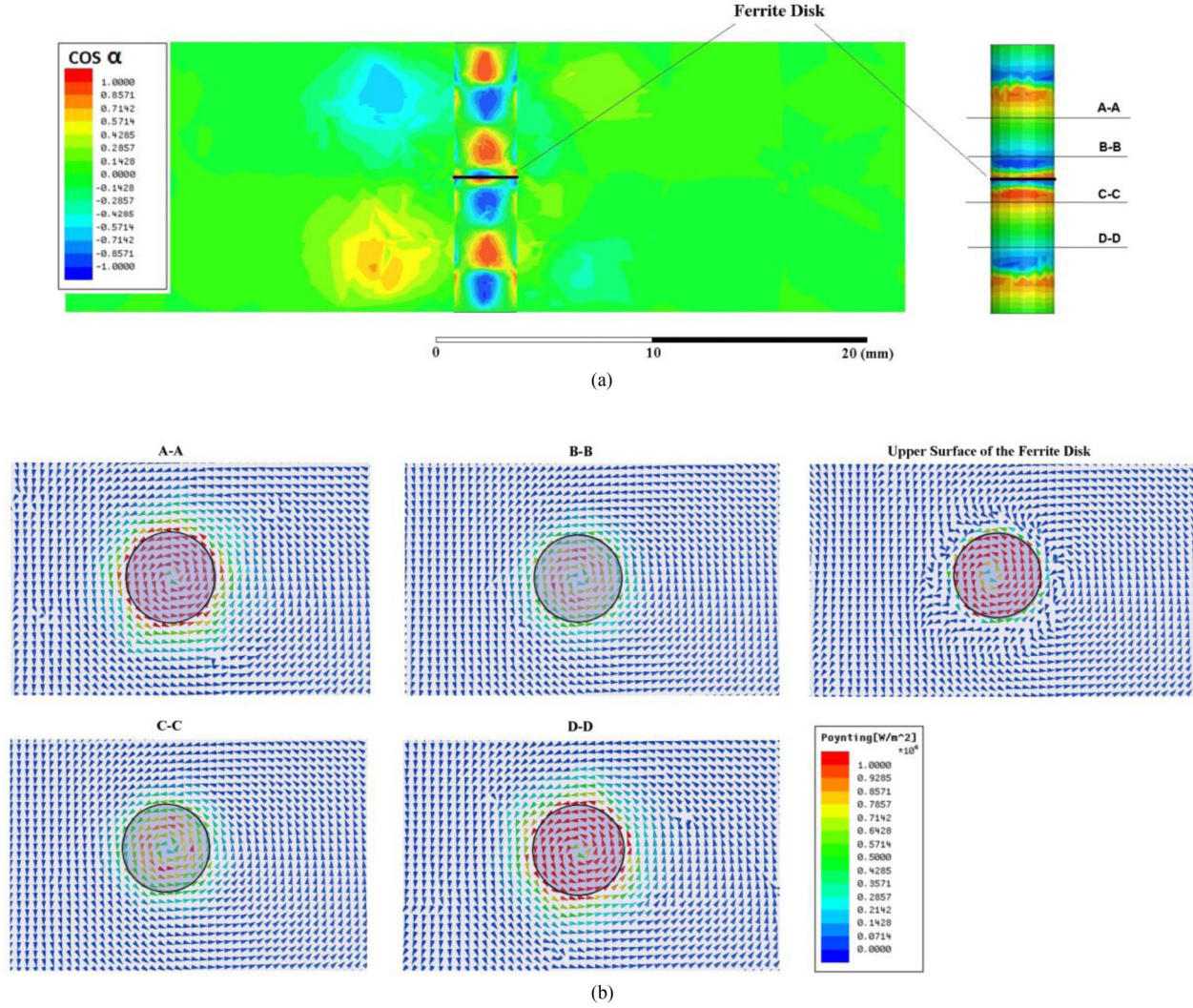
FIG. 17. (Color online) The field structure outside a ferrite disk for the second transmission peak (peak 2″) at a dielectric-cylinder load ($\varepsilon_r = 100$). (a) Normalized helicity parameter shown on the yz cross-section plane and on a lateral surface of a dielectric cylinder. (b) Power-flow distributions on planes A-A, B-B, C-C, and D-D, and immediately above a ferrite disk.
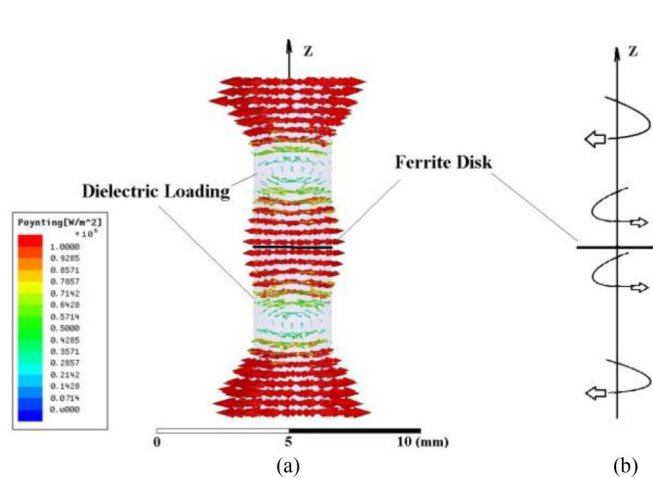

FIG. 18. (Color online) (a) An axial distribution of the power flow on a lateral surface of a dielectric cylinder ($\varepsilon_r = 100$) for the first transmission peak (peak 1″). (b) Schematic picture showing directions of rotations of the power-flow vortices along a cylinder axis.

parameter showing space angle between rotating vectors $\vec{E}$ and $\vec{H}$. In the regions where this parameter is not equal to zero, a space angle between the vectors $\vec{E}$ and $\vec{H}$ is not equal to 90°. The angle between rotating vectors $\vec{E}$ and $\vec{H}$ can vary in time, but remains unequal to 90° during a time period of microwave radiation. Figure 19 illustrates the ME-field topologies by schematic pictures of space curvature. There are the field topologies for the first MDM resonance (resonance peak 1′) at vacuum environment and for the second transmission peak (peak 2″) at a dielectric loading ($\varepsilon_r = 100$). The grids show coordinate systems in relation to mutual orientations of the $\vec{E}$ and $\vec{H}$ fields at a certain time phase. Suppose that the electric field $\vec{E}$ is directed along a basic vector $\vec{e}_1$ and the magnetic field $\vec{H}$ is directed along a basic vector $\vec{e}_2$. If the helicity parameter of the field is zero the dot product $\vec{e}_1 \cdot \vec{e}_2$ is zero as well. However, in a region where the helicity parameter of the field is not zero, the dot product $\vec{e}_1 \cdot \vec{e}_2$ does not vanish. There is a curved-space region. In a curved space, the electric and magnetic energies become coupled. There should exist a
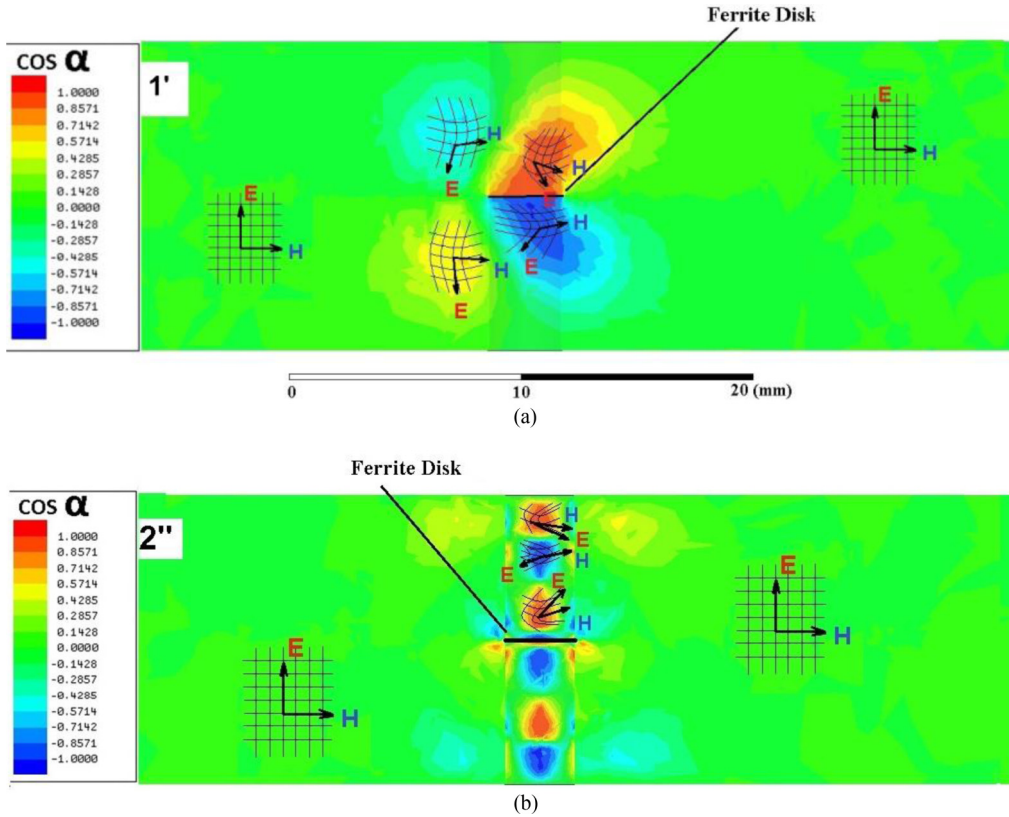
FIG. 19. (Color online) The ME-field topology is well illustrated by the space-time curvature. (a) Field topology for the first MDM resonance (resonance peak 1′) at vacuum environment. A vacuum cylinder ($\varepsilon_r = 1$) is shown as a highlighted area. (b) Field topology for the second transmission peak (peak 2″) at a dielectric loading ($\varepsilon_r = 100$). The angle between rotating vectors $\vec{E}$ and $\vec{H}$ can vary in time, but remains unequal to 90° during a time period of microwave radiation.

certain (magnetoelectric) mechanism of this coupling. In such a sense, ME fields can be considered as a Lorentz-violating extension of the Maxwell equations [12,13]. It seems likely that the Maxwell electrodynamics does not accurately describe what happens at a localized region of a MDM ferrite disk. A MDM ferrite disk appears as a real singularity for Maxwell electrodynamics, not a coordinate singularity. This singularity suggests that in the vicinity of a MDM ferrite disk the Maxwell electrodynamics is an incomplete theory.

A MDM vortex is a nonperturbative, nontrivial solution of the field equations. From Einstein's theory of general relativity it is well known that laws of physics that describe acceleration could also be used to describe gravity. It means that a MDM ferrite disk with vortex dynamics (in which originates the space-time curvature of the vacuum fields) can appear as an inertial mass. The problem of the vortex mass was discussed extensively over the years. In particular, the vortex inertial mass is considered as a significant effect in the superconductor theory [39,40]. At the same time, the concept of the vortex mass remains a controversial issue [41,42].

V. CONCLUSION

We showed that the spectra of MDM oscillations are very sensitive to material parameters of dielectric samples loading a ferrite disk. We found that topology of ME fields is strongly correlated with the Fano-resonance spectra observed

at terminals of a microwave structure. We observe the Fano-dipole and Fano-quadrupole spectra and also overlapping of Fano resonances. There exist specific thresholds in the Fano-resonance spectra appearing at certain permittivity parameters of dielectric samples. Importantly, different Fano resonances have different helicity properties of ME fields. The ME fields that originated from MDM ferrite disks are distinguished by topological portraits of the helicity parameters and can have a torsion degree of freedom.

The ME-field phenomena can be viewed as means of engineering of unique fields by artificial structures. Presently, the engineering of these fields by metamaterials is a topical subject. This concerns, in particular, the space-time coordinate transformations technique for invisibility cloak [37,38] and isotropic radiation [43], toroidal-multipole electromagnetic excitations [44], and optical superchiral fields [45]. The results obtained in this paper open vistas in the near- and far-field manipulation of microwave radiation. MDM oscillations, having both orbital and spin angular momenta, can twist microwave radiation. Due to a helical structure of ME fields, the effective cross section for microwave radiation is strongly increased. In the near-field applications, we propose alternative microwave sensors for material characterization, biology, and nanotechnology. Strong energy concentration and unique topological structures of the near fields originated from the MDM resonators allow effective measuring of chiral properties of materials in microwaves [11,15]. Generating far-field orbital

angular momenta from near-field microwave chirality of MDM structures can be a subject of great interest. Realization of such vortex generators opens the perspective for far-field microwave systems with topological-phase modulation [46].

[1] L. D. Landau and E. M. Lifshitz, *Electrodynamics of Continuous Media*, 2nd ed. (Pergamon, Oxford, 1984).

[2] A. I. Akhiezer, V. G. Bar'yakhtar, and S. V. Peletminskii, *Spin Waves* (North-Holland, Amsterdam, 1968).

[3] A. Gurevich and G. Melkov, *Magnetic Oscillations and Waves* (CRC Press, New York, 1996).

[4] D. D. Stancil and A. Prabhakar, *Spin Waves: Theory and Applications* (Springer, Berlin, 2009).

[5] E. O. Kamenetskii, Phys. Rev. E **63**, 066612 (2001).

[6] E. O. Kamenetskii, M. Sigalov, and R. Shavit, J. Phys.: Condens. Matter **17**, 2211 (2005).

[7] E. O. Kamenetskii, J. Phys. A: Math. Theor. **40**, 6539 (2007).

[8] E. O. Kamenetskii, J. Phys.: Condens. Matter **22**, 486005 (2010).

[9] E. O. Kamenetskii, M. Sigalov, and R. Shavit, Phys. Rev. A **81**, 053823 (2010).

[10] E. O. Kamenetskii, R. Joffe, and R. Shavit, Phys. Rev. A **84**, 023836 (2011).

[11] E. O. Kamenetskii, R. Joffe, and R. Shavit, Phys. Rev. E **87**, 023201 (2013).

[12] V. A. Kostelecký and M. Mewes, Phys. Rev. D **66**, 056005 (2002).

[13] M. Mewes and A. Petroff, Phys. Rev. D **75**, 056002 (2007).

[14] M. Berezin, E. O. Kamenetskii, and R. Shavit, J. Opt. **14**, 125602 (2012).

[15] R. Joffe, E. O. Kamenetskii, and R. Shavit, J. Appl. Phys. **113**, 063912 (2013).

[16] J. D. Jackson, *Classical Electrodynamics*, 2nd ed. (Wiley, New York, 1975).

[17] F. Wilczek, Phys. Rev. Lett. **58**, 1799 (1987).

[18] L. Visinelli, arXiv:1111.2268 (2011).

[19] M. Sigalov, E. O. Kamenetskii, and R. Shavit, J. Appl. Phys. **104**, 053901 (2008).

[20] E. O. Kamenetskii, A. K. Saha, and I. Awai, Phys. Lett. A **332**, 303 (2004).

[21] E. O. Kamenetskii, G. Vaisman, and R. Shavit, J. Appl. Phys. **114**, 173902 (2013).

[22] A. C. Johnson, C. M. Marcus, M. P. Hanson, and A. C. Gossard, Phys. Rev. Lett. **93**, 106803 (2004).

[23] G. Garcia-Calderon, R. Romo, and A. Rubio, Phys. Rev. B **47**, 9572 (1993).

[24] Z.-a. Shao and W. Porod, Phys. Rev. B **51**, 1931 (1995).

[25] Y. S. Joe, A. M. Satanin, and G. Klimeck, Phys. Rev. B **72**, 115310 (2005).

[26] E. O. Kamenetskii, J. Appl. Phys. **105**, 093913 (2009).

[27] M. Sigalov, E. O. Kamenetskii, and R. Shavit, J. Phys.: Condens. Matter **21**, 016003 (2009).

[28] E. O. Kamenetskii, M. Sigalov, and R. Shavit, J. Appl. Phys. **105**, 013537 (2009).

[29] R. A. Waldron, Q. J. Mech. Appl. Math. **11**, 438 (1958).

[30] F. W. Hehl, P. von der Heyde, G. D. Kerlick, and J. M. Nester, Rev. Mod. Phys. **48**, 393 (1976).

[31] R. T. Hammond, Rep. Prog. Phys. **65**, 599 (2002).

[32] W.-T. Ni, Rep. Prog. Phys. **73**, 056901 (2010).

[33] L. A. Turski and M. Mińkowski, J. Phys.: Condens. Matter **21**, 376001 (2009).

[34] A. Randono and T. L. Hughes, Phys. Rev. Lett. **106**, 161102 (2011).

[35] T. Van Doorsselaere, V. M. Nakariakov, and E. Verwichte, Astrophys. J. **676**, L73 (2008).

[36] H. K. Moffatt and R. L. Ricca, Proc. R. Soc. London, Ser. A **439**, 411 (1992).

[37] J. B. Pendry, D. Schurig, and D. R. Smith, Science **312**, 1780 (2006).

[38] U. Leonhardt and T. G. Philbin, New J. Phys. **8**, 247 (2006).

[39] M. W. Coffey and J. R. Clem, Phys. Rev. B **44**, 6903 (1991).

[40] D. Golubchik, E. Polturak, and G. Koren, Phys. Rev. B **85**, 060504(R) (2012).

[41] D. J. Thouless and J. R. Anglin, Phys. Rev. Lett. **99**, 105301 (2007).

[42] E. B. Sonin, Phys. Rev. B **87**, 134515 (2013).

[43] P.-H. Tichit, S. N. Burokur, C.-W. Qiu, and A. de Lustrac, Phys. Rev. Lett. **111**, 133901 (2013).

[44] T. Kaelberer, V. A. Fedotov, N. Papasimakis, D. P. Tsai, and N. I. Zheludev, Science **330**, 1510 (2010).

[45] E. Hendry, T. Carpy, J. Johnston, M. Popland, R. V. Mikhaylov-skiy, A. J. Lapthorn, S. M. Kelly, L. D. Barron, N. Gadegaard, and M. Kadodwala, Nat. Nanotechnol. **5**, 783 (2010).

[46] E. O. Kamenetskii, R. Joffe, M. Berezin, G. Vaisman, and R. Shavit, Prog. Electromagn. Res. B **56**, 51 (2013).